

The characterization of the interfacial interaction between polymeric methylene diphenyl diisocyanate and aluminum: A ToF-SIMS and XPS study[†]

Kyoko Shimizu,^{a*} Christopher Phanopoulos,^b Raf Loenders,^b Marie-Laure Abel^a and John F. Watts^a

Time of flight secondary ion mass spectrometry (ToF-SIMS) and X-ray photoelectron spectroscopy (XPS) have been employed to study the interfacial interaction between polymeric methylene diphenyl diisocyanate (PMDI) and aluminum produced by the deposition of a thin PMDI layer on the aluminum, in order to improve adhesion and/or abhesion performance.

When the PMDI concentration increases, the intensity ratio fragments indicative of the reaction product with water ($m/z = 106$ u: $C_7H_8N^+$) to that of isocyanate group ($m/z = 132$ u: $C_8H_6NO^+$) decreases. A very thin MDI layer on oxidized aluminum samples exhibits lower 106/132 ratio than degreased samples as a result of less hydroxide/hydroxyl species on the surface. This suggests that water reactions occur both at the surface of PMDI and at the PMDI/aluminum interface. The variation of the PMDI chemistry has also been studied by exposing PMDI treated samples to the air for various periods of time (a few hours to 14 days), in order to assess the reaction of the PMDI surface and PMDI/aluminum interface. At the interface, the yield of reaction with water is limited because of the finite amount of hydroxyl groups on the aluminum surface, and the water reaction is completed in a short period of time. However, the PMDI surface continues to react with water from the atmospheric. This methodology was also used to establish the presence of specific interactions at the PMDI/aluminum interface, and a fragment indicative of covalent bond formation between PMDI and aluminum ($AlCHNO_3^-$) is observed at the interface. Copyright © 2010 John Wiley & Sons, Ltd.

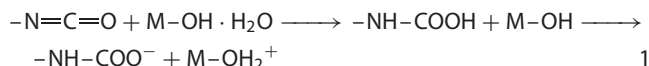
Keywords: isocyanate; polyurethane; aluminum; interface interaction; ToF-SIMS; XPS

Introduction

Polyurethane (PU) contains the urethane linkage ($-NHCOO-$) in its backbone chain, formed by the reaction of an isocyanate with a polyol. PUs exist in numerous forms ranging from flexible or rigid lightweight foams to tough, stiff elastomers.^[1] MDI-based polyurethanes are used in a wide range of applications: automotive, footwear, construction, furniture, thermal insulation, packaging industry, adhesives and coatings.^[1] In this work, the interface interaction between PMDI and aluminum has been studied using ToF-SIMS and XPS, in order to develop release options from aluminum moulds during the manufacture process and/or improve the adhesive performance for aluminum substrates.

The isocyanate group of PMDI reacts with compounds that contain active hydrogen groups such as hydroxyl, water, amine, urea and urethane, but also with other isocyanates. In the reaction with water, carbamic acid is produced, and the carbamic acid breaks down into amine and carbon dioxide. The amine then reacts with another isocyanate to form substituted urea, as shown in Fig. 1(a). The reaction of an isocyanate group with a hydroxyl group of polyol forms a urethane linkage (Fig. 1(b)). The isocyanate also reacts with urea to form biuret via active hydrogen (Fig. 1(c)), while the reaction with urethane forms allophanate (Fig. 1(d)). The isocyanates can react with themselves to form uretdione (dimer) (Fig. 1(e)) and isocyanurate (trimer) (Fig. 1(f)).

The isocyanate also produces carbodiimide and carbon dioxide by reacting with themselves and the carbodiimide slowly reacts with another isocyanate to form uretonimine (Fig. 1(g)). The high reactivity of isocyanate groups with active hydrogen is potentially the most important aspect of the interaction between isocyanates and metals. There are several assumptions in the mechanism of interaction between an isocyanate group and a metal surface.^[2–4] Dillingham *et al.* have studied the interface interaction between isocyanate based polymer and steel using Fourier transform infrared reflection (FT-IR) and the mechanism proposed is that the isocyanate functional groups can react with hydrated oxide on the metal surface to form carboxylate salts as shown below:^[2]



* Correspondence to: Kyoko Shimizu, Surrey Materials Institute and Faculty of Engineering & Physical Sciences, University of Surrey, Guildford, Surrey, GU2 7XH, UK. E-mail: k.shimizu@surrey.ac.uk

[†] Paper published as part of the SIMS Analysis of Polymers special issue.

^a Surrey Materials Institute and Faculty of Engineering & Physical Sciences, University of Surrey, Guildford, Surrey, GU2 7XH, UK

^b Huntsman, Everslaan 45, B-3078 Everberg, Belgium

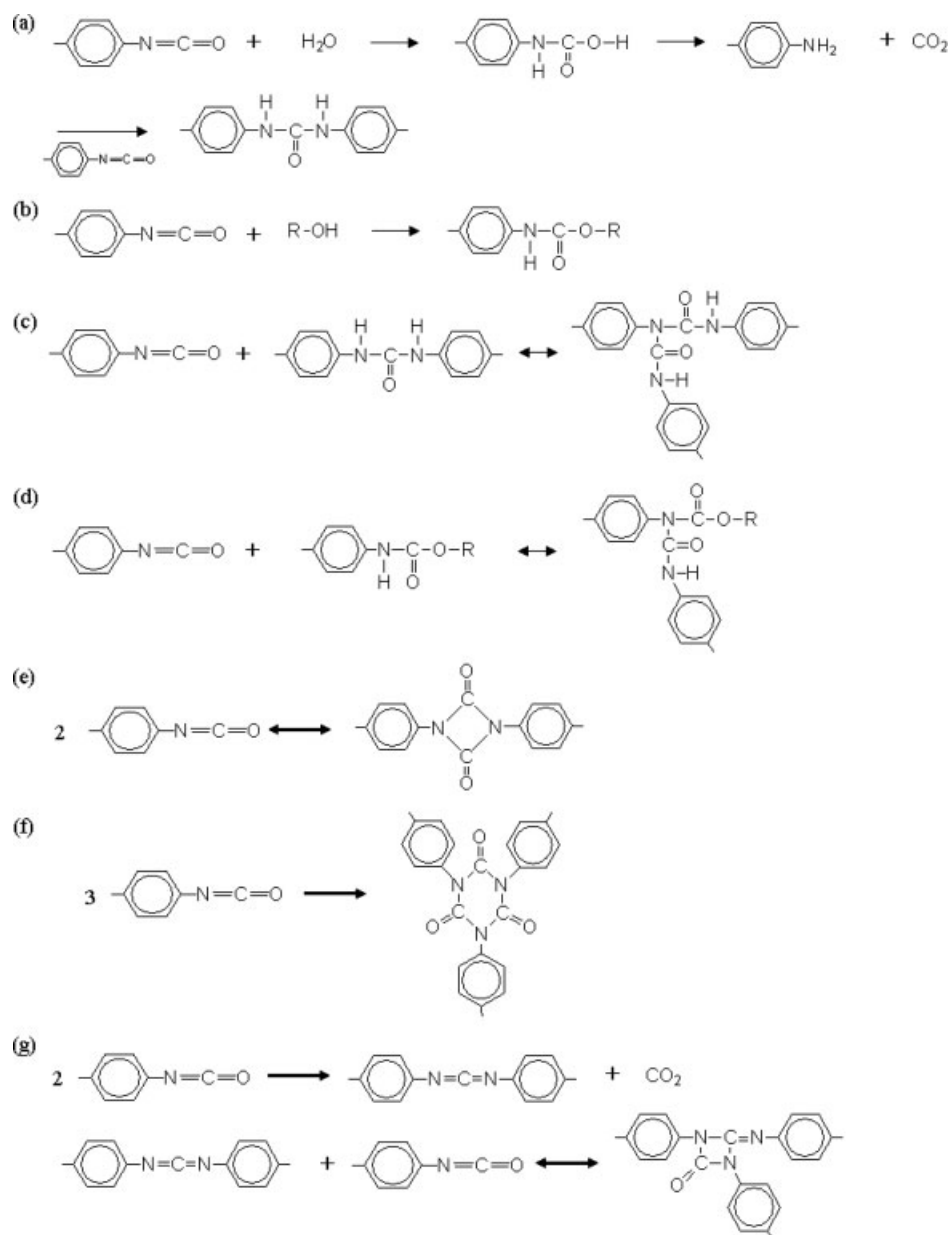


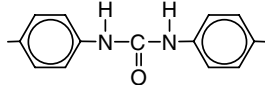
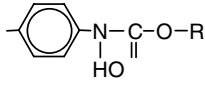
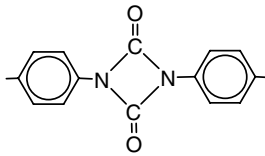
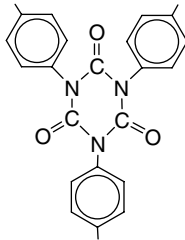
Figure 1. Synthesis of (a) urea, (b) urethane, (c) biuret, (d) allophanate, (e) uretdione, (f) isocyanurate, (g) carbodiimide and uretonimine formations.

where M is a metal. Subsequently, the carboxylate salts form covalent metal oxide–urethane linkages at higher temperature. Chehimi *et al.* have studied the interfacial reaction between aromatic moisture-cured urethane (ArMCU) and steel using XPS.^[3] They investigated the change in the oxide state of iron when ArMCU is deposited on the steel and suggested that covalent bonds are formed at the interface via hydroxyl groups from the steel surface, with a concomitant reduction of the oxidation state of iron. Kim *et al.* have studied an interface reaction between a phenyl isocyanate and an aluminum hydroxide surface using electrochemical tests and optical observation. They have deduced a reaction mechanism using molecular modeling.^[4] Both the electrochemical test and optical observation imply that the isocyanate functional group prefers to react with hydroxide aluminum. The charge distribution map of phenyl isocyanate, the negative charge on the nitrogen and oxygen and the positive

charge on the carbon of the isocyanate group, suggests that the nitrogen and carbon atoms of phenyl isocyanate favourably interact with hydrogen and oxygen atoms of hydroxide groups on aluminum surface, and this results in the formation of covalent bond via urethane linkage.

In this work, ToF-SIMS and XPS have been employed to study the interaction of PMDI with aluminum. ToF-SIMS can obtain the elemental and chemical information of the outermost molecular or atomic layer of a solid surface and the sensitivity is extremely high for all elements. XPS is utilized to determine all elements apart from H and He, and their chemical bonds. The information is obtained from the first few atomic layers and the detection limit is about 0.1 at.%. The combination of ToF-SIMS and XPS analysis techniques are particularly powerful for the comprehensive definition of polymer surface chemistry and the interaction of organic molecules with solid substrates. The aim of this work is to improve the knowledge

Table 1. Composition of reference samples

Sample	Reaction condition	Composition	Structure
High urea		·4, 4' diisocyanate + water	
High urethane	Cured for 2 h at 80 °C.	·51 g MDI (mixture 4,4 & 4,2 diisocyanate + 0.001% thionylchloride) ·43 g polyol (polyether + propylene oxide on sorbitol + 0.24% KOH) ·6 g Diolmix (59.4% tripropylene glycol + 18.6% monopropylene glycol + 22% butanediol 1,3) ·0.2 g Catalyst (67% mono ethyleneglycol + 33% triethylenediamine)	
High uretdione	Placed isocyanate in an oven for 2 weeks at 80 °C. Next, the precipitate was collected.	·98% 4, 4' diisocyanate	
High isocyanurate	Cured for 2 h at 80 °C.	·90 g polymeric MDI ·10 g polyol (polyether based on high ethylene oxide + low propylene oxide + glycol) ·4500 ppm catalyst (potassium 2-ethylhexanoate)	

of possible isocyanate–aluminum interactions. To this end, the interface interaction between PMDI and aluminum produced by deposition of a thin layer of PMDI on three different pretreated aluminum substrates has been studied. In order to assess the reaction of PMDI surface with atmospheric moisture and interface reaction between PMDI and aluminum, the variation of chemistry of PMDI on degreased aluminum has been examined by exposing the samples to ambient atmosphere for various periods of time.

Experimental

Sample preparation

Aluminum sheets (99.9% purity) were supplied by Chronos Ltd (Bedfordshire, UK). Samples of $10 \times 10 \text{ mm}^2$ were cut from 0.9-mm-thick aluminum sheets and subsequently cleaned with acetone using an ultrasonic bath to remove any organic contaminants. Then three different pretreated aluminum substrates, which are degreased, oxidized and hydrolyzed aluminum, were prepared with varied surface hydroxyl concentrations. The oxidized aluminum were made by heating in an oven at 220 °C for 2 h and then stored in a desiccator, while the aluminum was hydrolyzed by placing in boiling deionized water for 1 h.

PMDI (Suprasec 5025, Huntsman Holland BV, Rotterdam, The Netherlands) solution in the range of 10–0.01 vol.% in acetone were prepared to produce different thicknesses of PMDI adhesive layers on these different pretreated aluminum substrates. The PMDI solutions were deposited on these aluminum substrates by spin coating. Duplicate samples were prepared for ToF-SIMS and XPS analysis at each concentration. The samples were left in

ambient atmosphere (at room temperature and relative humidity are between 55 and 85%), for various periods of time (a few hours to 14 days) in order to assess the reaction of the PMDI surface with moisture from atmosphere, in comparison to the reaction at the interface between PMDI and aluminum.

Standard samples of high concentration of urea, urethane, uretdione and isocyanurate were prepared by Huntsman PU, and compositions and structures of these samples are shown in Table 1. High urethane and high isocyanurate samples were cut to expose fresh inside surfaces. High urea and high uretdione samples were supplied in powder form. The high urea samples were compressed to pellets, while the high uretdione samples were prepared for analysis by placing the powder on an aluminum coupon. Undiluted MDI was also examined by ToF-SIMS.

XPS analysis

XPS analysis was achieved using a modified ESCALAB MKII spectrometer (Thermo Fisher Scientific, East Grinstead, UK). The electron energy analyzer of the ESCALAB was updated to a Thermo Alpha 110 type. The analyzer was operated in the constant analyzer energy (CAE) mode at a pass energy of 100 eV for the survey spectra, and a pass energy of 20 eV for high-resolution spectra of the elements of interest. A nonmonochromated (twin anode) Al K α radiation with an energy 1486.6 eV at power of 300 W was used. The analysis area was ca. 6 mm in diameter. As is usual with twin anode XPS no additional charge compensation was employed, and a binding energy (BE) of 285.0 eV for the C–C/C–H components of C1s peak has been used as reference for charge correction. Spectral processing was carried out using the manufacture's software Advantage (v.4.37). The surface compositions are obtained from the

high-resolution spectra using sensitivity factors and transmission function correctly supplied with the Avantage datasystem.

ToF-SIMS analysis

ToF-SIMS analysis was achieved using a TOF.SIMS 5 (ION-TOF GmbH, Münster, Germany). Static SIMS conditions with a total ion dose less than 1×10^{13} ions cm^{-2} analysis $^{-1}$ were employed using a 9.5 keV Bi_3^+ primary ion beam operating in the high current bunched mode for high spectral resolution.^[5] An analysis area of $100 \times 100 \mu\text{m}^2$ at a resolution of 64×64 pixels was used. ToF-SIMS spectra were acquired over a mass range of 1–850 u in both positive and negative ion modes. Charge compensation was achieved using a pulsed electron flood source. Fragments of known composition, such as H^+ , CH_3^+ , Na^+ , H^- , C^- , O^- and OH^- were used for mass calibration and carefully checked these peak shapes did not have any charging effect. In addition, characteristic aluminum and PMDI fragments were also used.

The ToF-SIMS intensities for particular fragment ions under consideration are evaluated using the concept of their relative peak intensity (RPI), which is the ratio of the intensity of the ion of interest relative to the total ion intensity from $m/z = 0$ to 850 u:^[6]

$$\text{RPI}_x = I_x / I_{\text{total}} \quad 2$$

where x is the ion of interest and I_{total} is the total ion intensity between $m/z = 1$ and 840 u, and I_x is the measured intensity of the ion under consideration.

Peak-fitting of the high resolution ToF-SIMS spectra of nominal mass 102 was carried out using the computer software CasaXPS (v.2.3.16) provided by Casa Software Ltd (Teignmouth, UK).^[7–8] The line shape used was a numerical convolution of a Lorentzian

with a Gaussian, and the asymmetry index (a) is given by:

$$a = 1 - (\text{HWHM}_{\text{right}} / \text{HWHM}_{\text{left}}) \quad 3$$

where $\text{HWHM}_{\text{right}}$ and $\text{HWHM}_{\text{left}}$ are the half width at half maximum of the right and left asymmetric side of peak, respectively.

The accuracy of mass assignment, Δ (in ppm), is given by:^[9–10]

$$\Delta = |M_{\text{mea}} - M_{\text{ex}}| / M_{\text{ex}} \quad 4$$

Table 2. XPS surface composition of three different pretreated aluminum substrates

Sample	Surface concentration (at. %)			
	Al	O	C	N
Degreased Al	14.1	42.9	42.4	0.5
Oxidized Al	22.3	55.9	21.8	–
Hydrolyzed Al	20.1	71.1	8.8	–

Table 3. Carbon functionalities with their binding energies of variable aluminum substrates

Sample	Surface concentration of C1s peak fitting (at.%) (The binding energies of peak fitting (eV))			
	C–C/C–H	C–O/C–OH	C=O	O–C=O
Degreased Al	31.6 (285.0)	6.3 (286.4)	1.3 (287.9)	2.6 (289.5)
Oxidized Al	14.1 (285.0)	3.5 (286.3)	1.5 (287.8)	2.6 (289.4)
Hydrolyzed Al	7.2 (285.0)	1.0 (286.4)	–	0.5 (288.8)

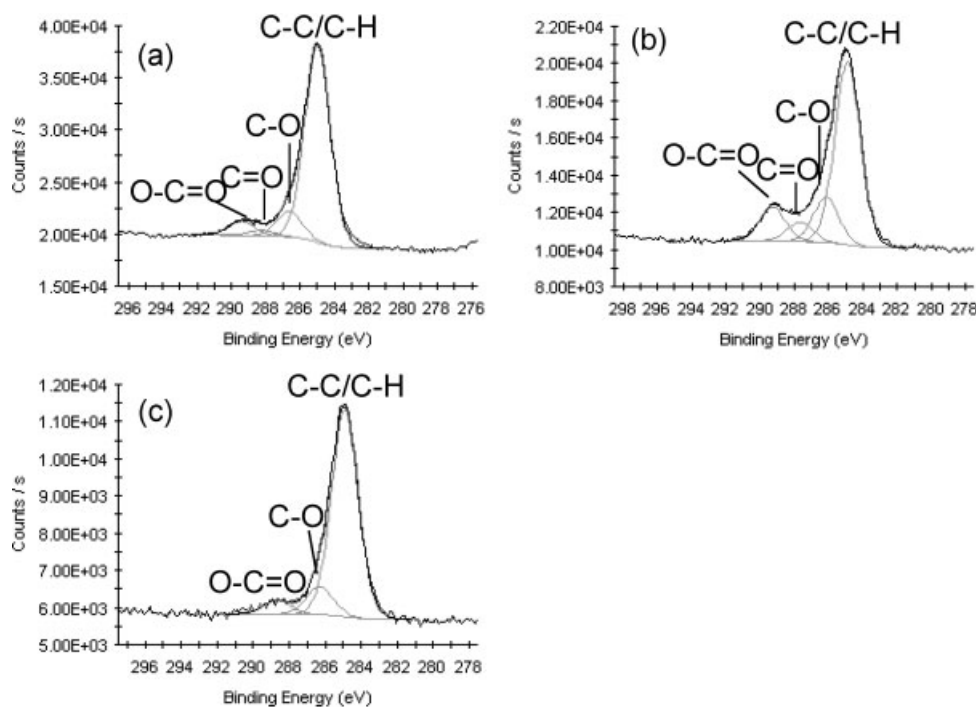


Figure 2. C1s peak fitting of (a) degreased, (b) oxidized and (c) hydrolyzed aluminum.

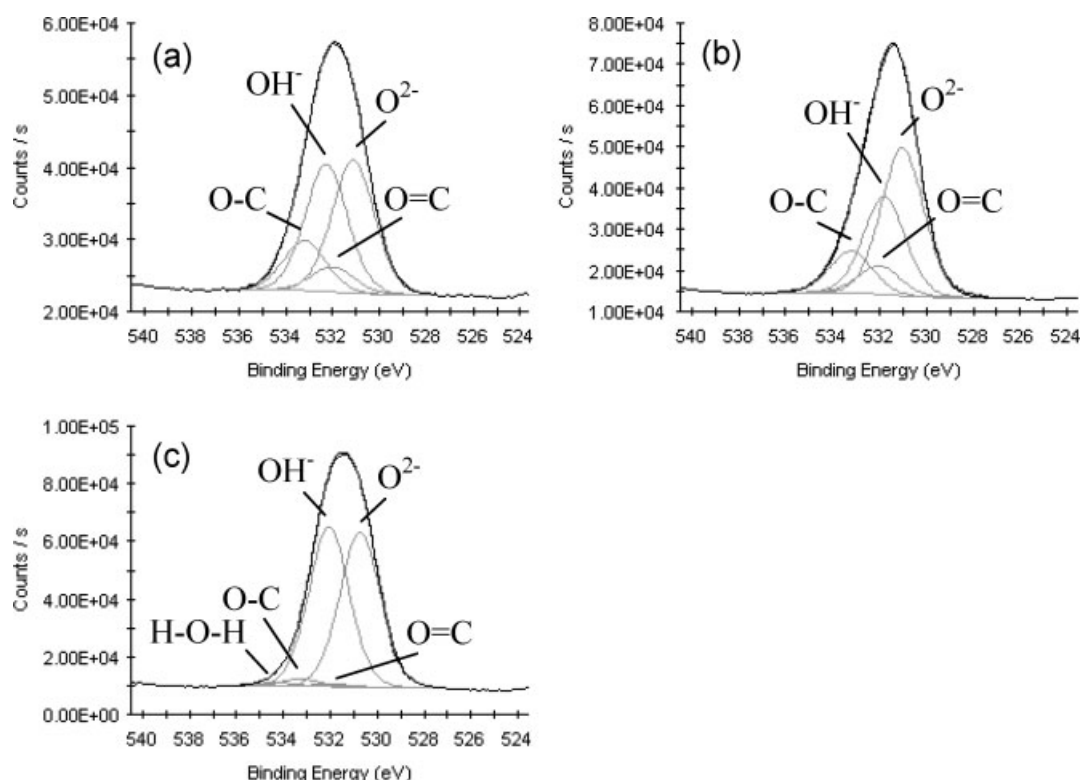


Figure 3. O1s peak fitting of (a) degreased, (b) oxidized and (c) hydrolyzed aluminum.

Table 4. Oxygen functionalities with their binding energies of variable aluminum substrates

Sample	Surface concentration of O1s peak fitting (at.%) (The binding energies of peak fitting (eV))					
	Al-O	Al-OH	H-O-H	C=O	C-O	Al-OH /Al-O
Degreased Al	17.1 (531.2)	16.5 (532.3)	–	3.2 (532.0)	6.4 (533.2)	0.96
Oxidized Al	26.3 (531.2)	17.4 (531.9)	–	5.0 (532.1)	7.5 (533.3)	0.66
Hydrolyzed Al	33.9 (530.8)	35.0 (532.1)	0.5 (534.4)	0.6 (532.1)	1.6 (533.4)	1.03

where M_{mea} is the measured mass obtained from high-resolution spectrum, and M_{ex} is the exact mass of the molecules.

Results and Discussion

XPS analysis

Aluminum surface after pretreatments

The surface compositions of three different pretreated aluminum surfaces are shown in Table 2. Degreased aluminum exhibits a relatively high carbon concentration with a low concentration of aluminum and oxygen, compared with oxidized and hydrolyzed samples. The carbon signal has decreased while aluminum and oxygen signals are increased both after oxidation and hydration. The carbon originates mainly from hydrocarbon, but also oxygen and hydroxyl functionalized carbon are observed.

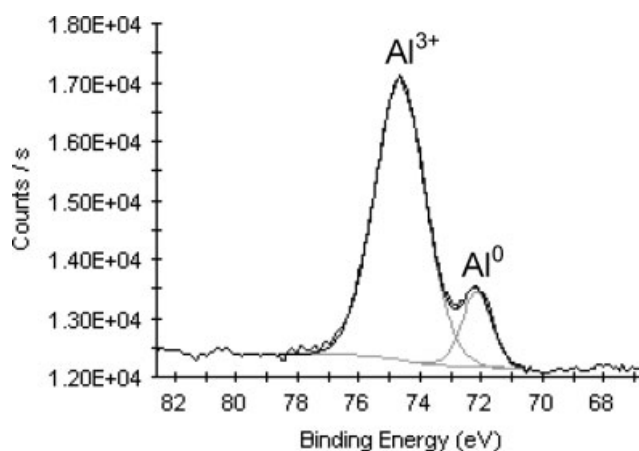


Figure 4. Al2p peak fitting of degreased aluminum.

Four components, C-C/C-H (BE = 285.0 eV), C-O/C-OH, (BE = 286.3–286.4 eV), C=O (BE = 287.8–287.9 eV) and O-C=O (BE = 288.8–289.5 eV), were used in the C1s peak fits, as shown in Fig. 2 and Table 3.^[11–13] The adventitious hydrocarbon is evaporated upon heating. By contrast, the adventitious carbon is desorbed from aluminum surface to the boiling deionized water. When the aluminum substrate is taken out from the boiling deionized water, the aluminum surface has high surface-free energy and, hence, the adventitious hydrocarbon is adsorbed on the surface. By hydration, the aluminum surface becomes porous as a result of a formation of pseudoboehmite,^[6,14–15] and, hence, more surface area leads to the reduction of the adventitious carbon concentration compared with the degreased substrate. Since O=C (BE = 532.0–532.1 eV) and O-C (BE = 533.2–533.6 eV) components

Table 5. Aluminum functionalities with their binding energies of variable aluminum substrates

Sample	Surface concentration of Al2p peak fitting (at.%) (The binding energies of peak fitting (eV))		
	Al ⁰	Al ³	Al ³ /(Al ⁰ + Al ³)
Degreased Al	2.0 (72.2)	12.1 (74.7)	0.86
Oxidized Al	4.1 (72.0)	18.0 (74.7)	0.81
Hydrolyzed Al	–	20.1 (74.2)	1.00

Table 6. XPS surface composition of variable concentration PMDI-treated aluminum

pMDI concentration (vol.%)	Surface concentration (at.%)			
	C	N	O	Al
Degreased aluminum	42.4	0.5	42.9	14.1
0.01	30.3	1.3	50.3	18.1
0.05	47.3	3.9	36.9	11.9
0.1	51.7	5.6	31.8	10.9
0.25	64.3	9.4	20.5	5.8
0.5	65.4	8.9	20.2	5.6
1	68.0	10.2	17.4	4.4
5	72.1	11.2	14.3	2.5
10	72.8	11.3	13.6	2.3

can also be observed in the O1s peaks, the cross reference of C1s and O1s peak fits allow to quantify aluminum oxide (O^{2−}) and hydroxide (OH[−]) components of O1s. C–C/C–H peak at 285.0 eV has been used as reference for charge correction, however, this correction is not appropriate to use for aluminum oxide/hydroxide because there is a vertical differential charge between adventitious carbon layer and aluminum oxide/hydroxide surface, and hence, a shift in the aluminum oxide/hydroxide of Al2p and O1s peaks are independent from the C1s peak.^[16–18] In order to determine the position of O^{2−}, OH[−] and H₂O, the separations between these components of O1s and the Al³⁺ of Al2p peaks are calculated to be 456.5–456.6 eV, 457.2–457.9 eV and 460.3 eV, respectively.^[16–17] The O1s peak fit shows that the hydroxide aluminum surface has the highest amount of hydroxide groups on the surface, while surface of oxidized aluminum has the lowest hydroxide concentration, as shown in Fig. 3 and Table 4. The Al2p peak fits reveal only Al³⁺ for the hydrolyzed aluminum, whereas both Al⁰ and Al³⁺ are present in the degreased and the oxidized aluminum substrates,

as shown in Fig. 4 and Table 5. A thick pseudoboehmite (AlOOH) layer is formed by hydration^[14–17] and the pseudoboehmite layer is much thicker than oxy/hydroxyl layer of degreased and oxidized aluminum. The degreased and the oxidized aluminum substrates exhibit similar Al³⁺/(Al⁰ + Al³⁺) ratios, 0.86 and 0.81, respectively. However, the oxidized aluminum exhibits thinner carbonaceous layer on the surface than the degreased aluminum, and hence, the detection of aluminum signal is deeper than the degreased sample. In this case, the oxide layer of oxidized aluminum is assumed to be thicker than that of degreased aluminum.

MDI deposited on aluminum substrate

XPS analysis has been employed to estimate the variation of the PMDI layer thickness on aluminum substrates, and to examine at which concentration the interface between PMDI

Table 7. Carbon functionalities with their binding energies of variable concentration PMDI-treated aluminum

PMDI concentration (vol.%)	Surface concentration of C1s peak fitting (at.%) (The binding energies of peak fitting (eV))				
	1st peak	2nd peak	3rd peak	4th peak	5th peak
	C–C/C–H	C–N/ C–O/C–OH	C=O	N=C=O/ N–CN=O/ N–COH=O/ O–C=O	Shake-up satellite
Degreased Al	37.8 (285.0)	4.9 (286.7)	1.1 (288.3)	2.7 (289.4)	–
0.01	20.9 (285.0)	5.1 (286.1)	1.9 (287.8)	2.5 (289.5)	–
0.05	37.7 (285.0)	5.8 (285.8)	–	3.9 (289.1)	–
0.1	* 38.4 (285.0)	9.2 (286.3)	–	4.2 (289.2)	(291.4)
0.25	* 48.9 (285.0)	10.5 (286.2)	–	4.9 (289.4)	–
0.5	* 49.6 (285.0)	11.0 (286.2)	–	4.9 (289.3)	(291.8)
1	* 51.2 (285.0)	11.7 (286.2)	–	5.1 (289.4)	–
5	* 54.1 (285.0)	12.4 (286.2)	–	5.6 (289.4)	(291.8)
10	* 54.1 (285.0)	13.2 (285.9)	–	5.4 (289.4)	–

* : Including shake-up satellite component

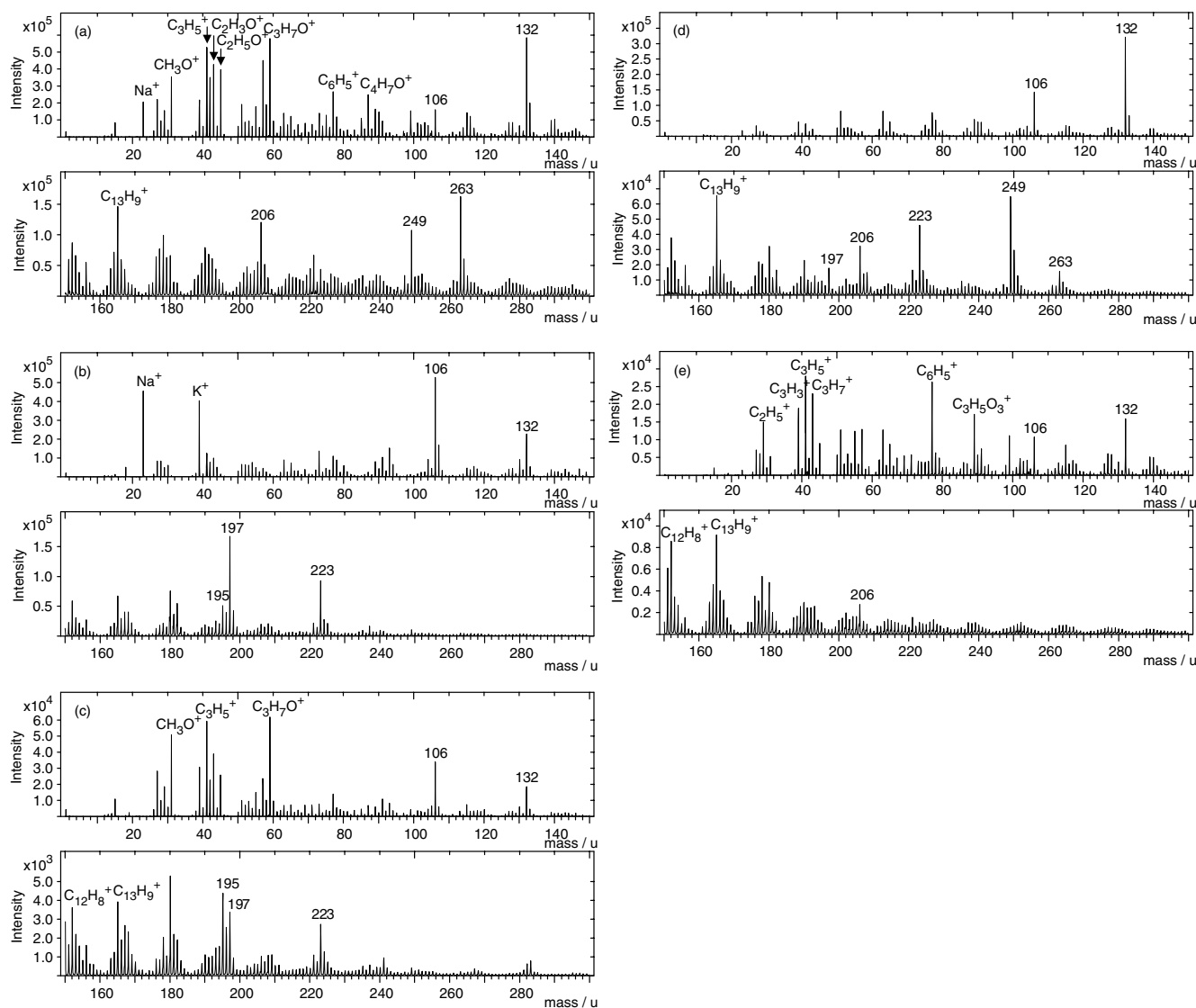


Figure 5. Positive ToF-SIMS spectra of reference samples: (a) PMDI, (b) high urea, (c) high urethane, (d) high uretdione and (e) high isocyanurate.

and aluminum substrates can be examined. Table 6 shows the surface composition of the degreased aluminum and PMDI treated aluminum samples. The degreased aluminum sample exhibits a slightly higher carbon concentration together with a lower concentration of oxygen and aluminum than the sample treated with 0.01 vol.% PMDI. This is probably a result of the displacement of adventitious carbon by a spin-cast PMDI coating. When the PMDI concentration increases, intensities of carbon and nitrogen increase while the intensity of aluminum decreases.

Table 7 shows the surface concentrations for the different chemical states of carbon established by peak fitting of the C1s core level spectra. The first C1s peak at BE 285.0 eV is assigned to hydrocarbon, C–C/C–H. The BE of the second peak between 285.8 and 286.7 eV is assigned to alcohol and/or ether carbon groups, C–O/C–OH, and C–N, the BE of the third peak ranges between 287.8 and 288.3 eV is assigned to carbonyl carbon, C=O, the BE of forth peak between 289.1 and 289.4 eV is assigned to acid and ester carbon groups, O–C=O, and N=C=O, N–CN=O and N–COH=O.^[3,11,19] The last peak present at high BE between 291.4 and 291.7 eV is due to a shake-up satellite

resulting from the $\pi \rightarrow \pi^*$ transition in the phenyl ring.^[11,20] As the concentration of MDI increases, all peak signals increase apart from C=O bonding. The BE of N=C=O, N–CN=O and N–CO=O components are similar with each other so these components cannot be distinguished from peak position. Theoretically, MDI has same ratio of C–N to N=C=O, while the ratio of C–N to N–CN=O increases as a result of formation of carbon dioxide. In this experiment, however, O–C=O component of adventitious carbon is greatly contributed as PMDI concentration decreases. Therefore, it is difficult to examine the interface reaction from C1s peak fitting.

Thickness of the carbonaceous layer can be calculated using the modified Beer-Lambert equation:^[20–21]

$$d = \lambda_c \cos \theta \ln (1 + D_{Al} \lambda_{Al} I_c / D_c \lambda_c I_{Al}) \quad 5$$

where d is the carbonaceous thickness, D_{Al} and D_c are the densities of the aluminum and carbon, λ_{Al} and λ_c are the attenuation length of the photoelectrons in the aluminum and in the carbon, I_{Al} and I_c are the intensities of the aluminum and the carbon, and θ is the photoelectron take-off angle to the surface normal (set at $\theta = 45^\circ$ for

Table 8. Thickness of carbonaceous layer of PMDI treated aluminum samples

PMDI concentration (vol.%)	Thickness (nm)		
	Degreased Al	Oxidized Al	Hydrolyzed Al
0.01	2.8		
0.05	4.1	4.0	1.9
0.1	4.4		
0.25	5.7	5.2	2.7
0.5	5.8		
1	6.3		
5	7.3	10.5	–
10	7.5		

these experiments). Densities of PMDI and aluminum are 1.23 and 2.7 g cm⁻³, respectively.^[22–23] The attenuation lengths of C1s and Al2p are 2.4 and 2.8 nm, respectively.^[21,24] The carbonaceous thicknesses of PMDI treated degreased aluminum samples are in a range of 2.8 to 7.5 nm as shown in Table 8. These thicknesses are appropriate to examine from the reaction of PMDI surface to the interface interaction between PMDI and aluminum using ToF-SIMS. 0.05 and 0.25 vol.% MDI-treated hydrolyzed aluminum samples has less carbonaceous layer than degreased and oxidized samples. By hydration, the porous surface is formed, and thus, the increase in surface area leads to the reduction of the carbonaceous layer thickness.

ToF-SIMS analysis

Reference samples

There are several reaction products of isocyanate as mentioned in the introduction. The most important reactions are with water, with hydroxyl groups and NCO/NCO reactions under a range of conditions and in the presence of different types of catalysts. Therefore, some of these possible reaction products are examined by ToF-SIMS in order to have references for the interpretation of the ToF-SIMS data relative to interface interaction between PMDI and aluminum. Figure 5 shows the positive ToF-SIMS spectra in the mass range of $m/z = 1–300$ u of the reference samples. From PMDI sample, at lower mass region, high intensities of Na⁺, CH₃O⁺, C₃H₅⁺, C₂H₃O⁺, C₂H₅O⁺, C₃H₇O⁺, C₆H₅⁺ and C₄H₇O⁺ are observed, and these are either MDI-derived fragments, and/or fragments of materials present in the PMDI production process. High intensities of fragments of isocyanate functional groups ($m/z = 132$, 206, 249 and 263 u) are observed in the PMDI sample. Low intensity of a fragment of an amine functional group ($m/z = 106$ u) is also observed, and this fragment probably originates from the reaction product of PMDI exposed to atmospheric moisture before the analysis so that there is a small yield of the water reaction product on the PMDI surface. A typical PMDI contains a mixture of di-iso (30–50 wt.%), tri-iso (20–30 wt.%) and small amounts of tetra, penta isocyanates and higher homologue.^[1,25] The tri-isocyanate component of PMDI is used to show possible PMDI origin fragments as shown in Fig. 6.^[26] Only one of the possible fragments at each mass is presented since there might be different charge localization and structures.

Table 9 suggests possible ion assignments for positive ion fragments originating from MDI as well as from its common reaction products.^[27–28] Both the amine group ($m/z = 106$ u) and the isocyanate group ($m/z = 132$ u) are observed in all reference

Table 9. Possible structures of positive ion fragments from the PMDI and related reaction products

Mass	Formula	Structure
77	C ₆ H ₅ ⁺	
91	C ₇ H ₇ ⁺	
106	C ₇ H ₈ N ⁺	
132	C ₈ H ₆ NO ⁺	
195	C ₁₃ H ₁₁ N ₂ ⁺	
197	C ₁₃ H ₁₃ N ₂ ⁺	
206	C ₁₄ H ₈ NO ⁺	
223	C ₁₄ H ₁₁ N ₂ O ⁺	
249	C ₁₅ H ₉ N ₂ O ₂ ⁺	
263	C ₁₆ H ₁₁ N ₂ O ₂ ⁺	

Table 10. The main characteristic fragments observed from the reference samples

Sample	Mass (u)									
	77	91	106	132	195	197	206	223	249	263
MDI	✓	✓	✓	✓	–	–	✓	–	✓	✓
High urea	✓	✓	✓	✓	✓	✓	–	✓	–	–
High urethane	✓	✓	✓	✓	✓	✓	–	✓	–	–
High uretdione	✓	✓	✓	✓	–	✓	✓	✓	✓	✓
High isocyanurate	✓	✓	✓	✓	–	–	✓	–	–	–

samples. The relative ratios of mass 106–132 u in the PMDI, high uretdione, high isocyanurate, high urethane and high urea samples are 0.1, 0.4, 0.5, 1.0 and 2.8, respectively. This high 106/132 ratio of high urethane and urea can be used as an indication of the formation of reaction products with hydroxyl groups and water for PMDI treated aluminum samples.

For the high urea and urethane samples, peaks of isocyanate groups ($m/z = 132$ u), amine groups ($m/z = 106$, 195 and 197 u) and both amine and isocyanate groups ($m/z = 223$ u) are observed. However, the relative intensities are different, for example, the ratio of fragments at mass 195 to 197 u for high urea and

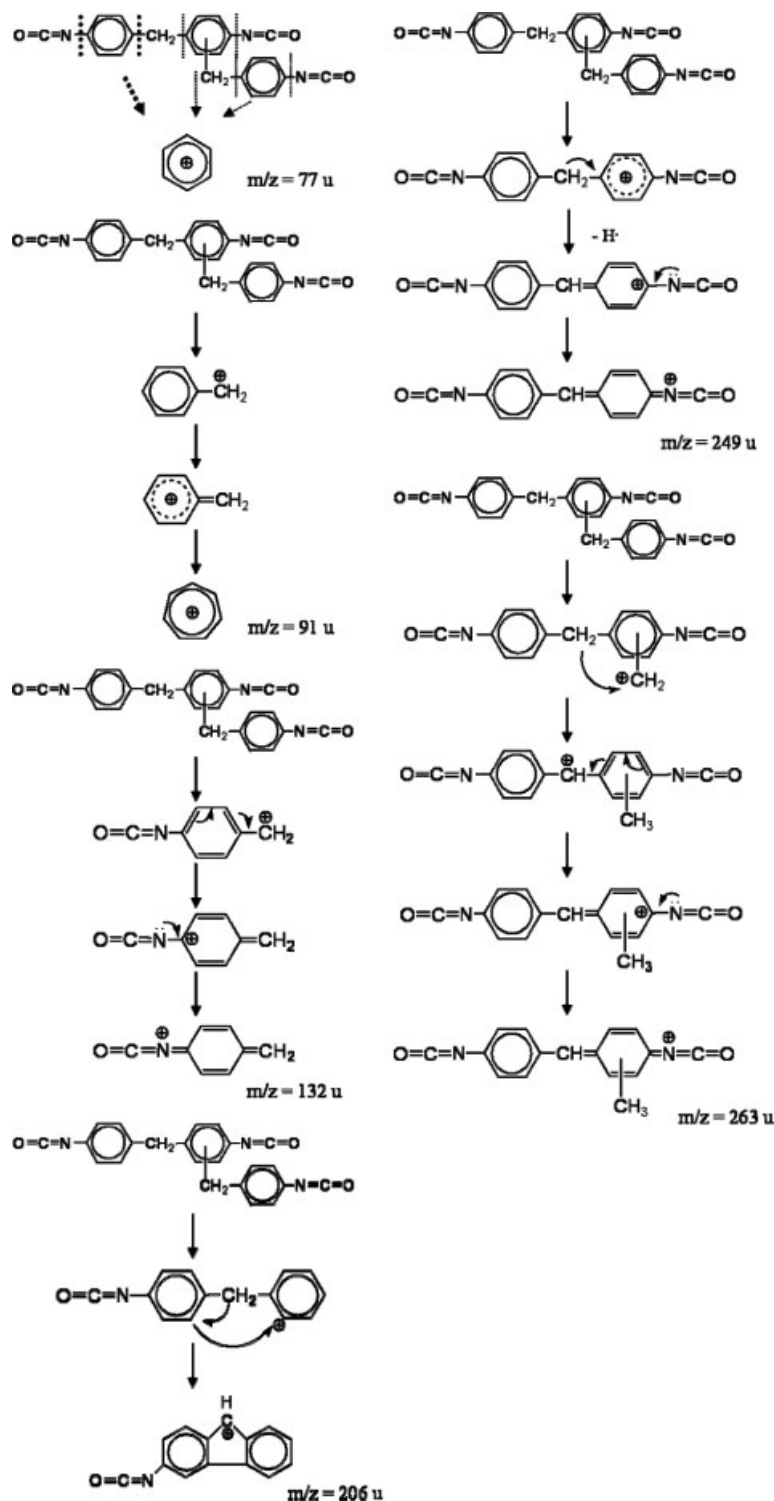


Figure 6. Fragmentation pattern of PMDI.

urethane samples are 0.4 and 1.6, respectively. A peak of high intensity, which has both isocyanate and amine functional groups ($m/z = 223$ u), and that of relatively low intensity, which has two amine groups ($m/z = 197$ u), are observed from the high uretdione sample. The intensity of the peak at mass 263 u is low compared with that of the PMDI sample while that of the peaks at mass 106 and 223 u are high. For the high isocyanurate sample,

fragments of isocyanurate groups ($m/z = 132$ and 206 u) and of amine groups ($m/z = 106$ u) are observed. Table 10 shows the summary of the main characteristic fragments observed from the reference samples. Overall, the PMDI and the high uretdione samples have fragments that contain many isocyanate groups whereas the high urea and urethane samples exhibited more amine groups, as may have been expected since the PMDI and

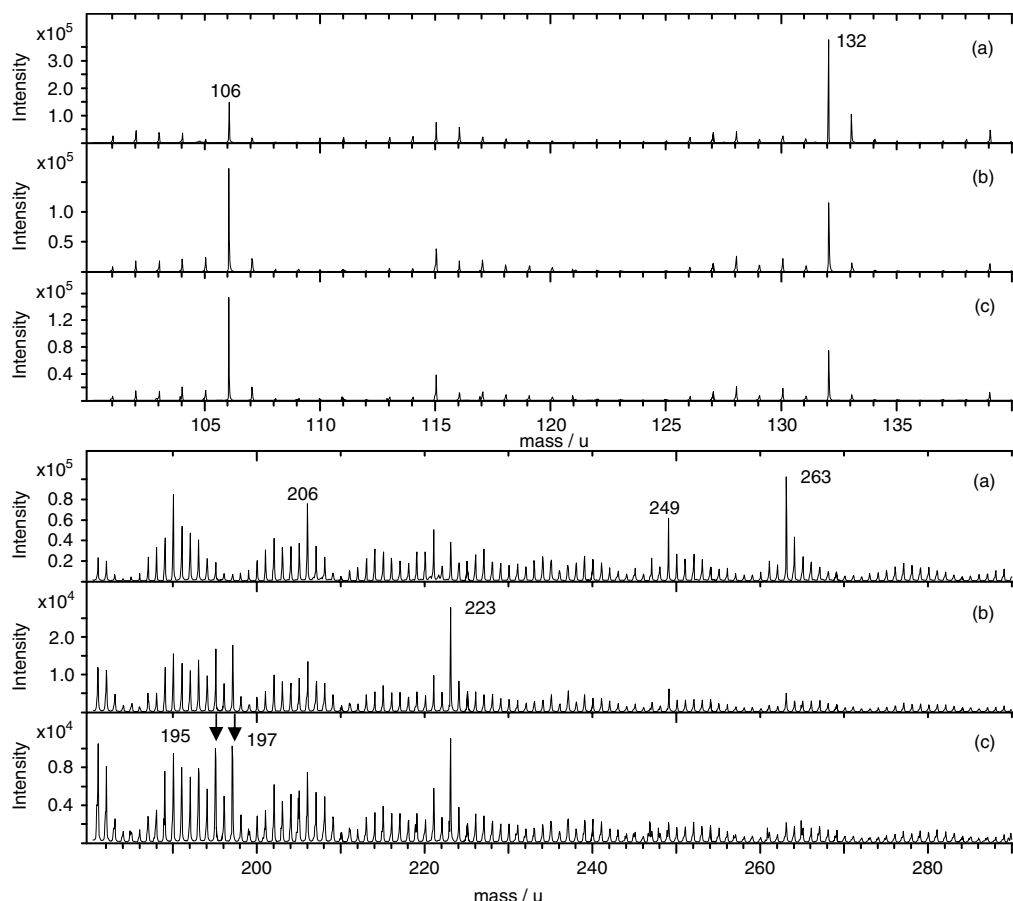


Figure 7. Positive ToF-SIMS spectra ($m/z = 100$ – 140 and 180 – 290 u) of degraded aluminum treated with (a) 5 vol.% PMDI (calculated film thickness: 7.3 nm), (b) 0.25 vol.% PMDI (calculated film thickness: 5.7 nm) and (c) 0.05 vol.% PMDI (calculated film thickness: 4.1 nm).

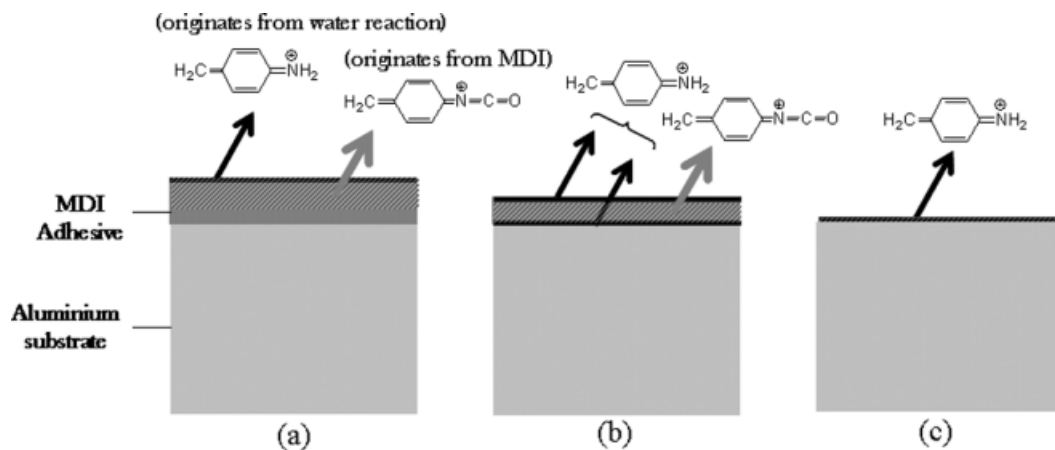


Figure 8. Schematic information (a) thick (>7.5 nm), (b) intermediate (4.1–7.4 nm) and (c) thin (<4.1 nm) PMDI layer on aluminum samples.

high uretdione materials are essentially unreacted NCO bearing materials, whilst the high urea and urethane products are formed by consuming the NCO groups by reaction with alcohols and water respectively.

MDI deposited on aluminum substrate

Figure 7 shows the positive ToF-SIMS spectra for different PMDI concentrations coated on degraded aluminum substrates in the mass range of 100–140 and 180–290 u. MDI-treated aluminum

samples were stored under vacuum of the ToF-SIMS introduction chamber within a few hours of preparation, in order to prevent a further reaction with atmospheric moisture. From 5 vol.% PMDI treated aluminum sample, high intensities of fragments containing isocyanate functional groups ($m/z = 132$, 206, 249 and 263 u), originating from PMDI, are observed. When PMDI concentration decreases, intensities of these fragments decrease while intensities of fragments ($m/z = 106$, 195, 197 and 223 u), originating from the reaction product of isocyanate with water, increase. Figure 8

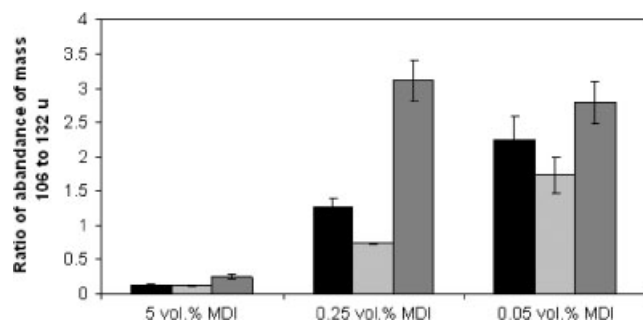


Figure 9. The ratio of the intensity of a fragment indicative of the reaction product with water ($m/z = 106$ u) to the intensity of isocyanate group ($m/z = 132$ u) of samples using different pretreated aluminum samples (left: degreased aluminum, middle: oxidized aluminum, right: hydrolyzed aluminum).

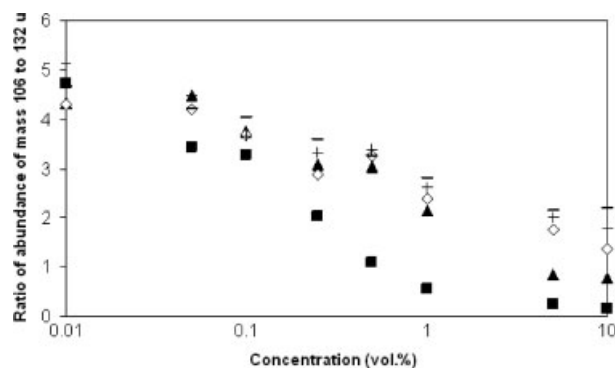


Figure 10. The ratio of the intensity of the fragment originating from the reaction product of isocyanate with water ($m/z = 106$ u) to that of the fragment originating from PMDI ($m/z = 132$ u) after exposure the PMDI treated degreased aluminum samples to air for various periods (■: a few hours, ▲: 2 days, ◇: 3 days, ⊕: 6 days, —: 14 days).

shows a schematic of the depth information of PMDI treated aluminum samples. A fragment originating from PMDI is observed on the PMDI surface and bulk. As PMDI thickness decreases, the fragment will be detected from only the PMDI layer. The surface of PMDI can react with water from atmospheric moisture and the water reaction also occurs at the interface between PMDI and aluminum via hydroxide groups on the aluminum surface.^[29–30] Therefore, a fragment which originates from water reaction is observed at the surface of PMDI and at the interface between PMDI and aluminum. For thick PMDI-coated samples, 10 and 5 vol.% PMDI treated samples have more than 7.5 nm thickness of the carbonaceous layer on the surface and Al^+ fragments ($m/z = 27$ u) are not observed from the spectra. The film is too thick to observe the interface, and hence, the all fragments are observed only from the PMDI surface and bulk. By contrast, Al^+ fragments are observed on less than 1 vol.% PMDI concentration samples and the intensity of Al^+ peak increases with reducing PMDI thickness. Therefore, the signals are observed from both the PMDI and the interface between PMDI and aluminum, and for very thin layer PMDI sample the signals are observed at the interface region, and are mainly reaction products both from hydroxide groups on the aluminum surface and from atmospheric moisture.

PMDI deposited in the oxidized and hydrolyzed aluminum substrates were examined to study the interface reaction in order to compare with PMDI-treated degreased aluminum samples. Figure 9 shows the ratio of the fragment at mass 106 u and 132 u

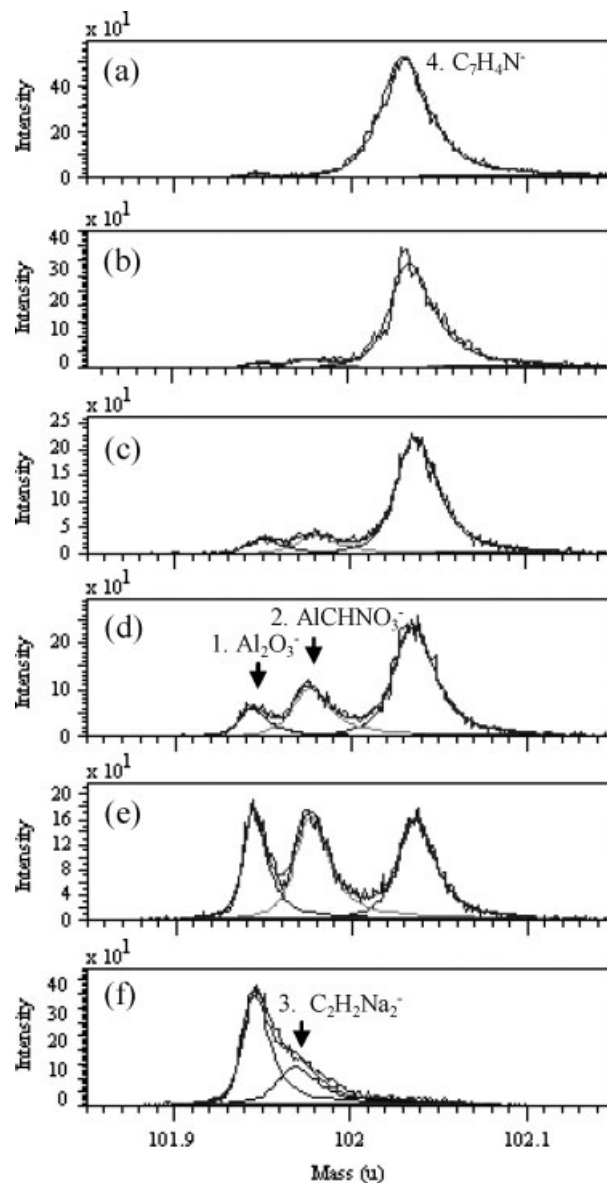


Figure 11. Spectra of nominal mass $m/z = 102$ u at high mass resolution of degreased aluminum treated with (a) 5 vol.%, (b) 0.5 vol.%, (c) 0.25 vol.%, (d) 0.1 vol.%, (e) 0.05 vol.% and (f) without PMDI.

of three different types of aluminum treated with variable PMDI concentration. 5 vol.% MDI treated degreased and oxidized samples exhibit similar 106/132 ratio, while the ratio is high on 5 vol.% treated hydroxide sample, and this is because surfaces of the samples treated by boiling in deionized water have a high surface area as a result of the interlocking acicular morphology^[6] so that 5 vol.% treated hydroxide sample has more surface area to react with atmospheric moisture than 5 vol.% MDI treated degreased and oxidized samples. For 0.25 and 0.05 vol.% samples, the 106/132 ratios of oxidized aluminum are lower than degreased samples. The carbonaceous thicknesses of oxidized samples are similar, or even thinner, than degreased samples so that the amount of reaction products from atmospheric moisture are similar with both samples, therefore, the differences can be the amount of reaction products with hydroxide groups in the aluminum surface, as a result of less hydroxide on the surface of oxidized aluminum substrate than degreased substrate. By contrast, the 106/132 ratios of

Table 11. Fragment obtained at nominal mass 102 and their respective assignment

Peak no.	Experimental mass (u)	Exact mass (u)	$ \Delta $ (ppm)	Formula
1	101.9434–101.9506	101.9478	6.9–43.2	Al_2O_3^-
2	101.9758–101.9793	101.9772	3.9–20.6	AlCHNO_3^-
3	101.9683	101.9694	10.8	$\text{C}_2\text{O}_2\text{Na}_2^-$
4	102.0289–102.0364	102.0344	2.9–53.9	$\text{C}_7\text{H}_4\text{N}^-$

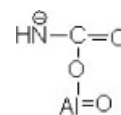
hydrolyzed samples are high compared with degreased samples. This is because PMDI layers are thinner than degreased aluminum as a result of the formation of porous surface by hydration, and also more reaction product with hydroxide groups might be produced due to higher concentration of hydroxide groups on the surface than degreased aluminum surface.

PMDI-treated aluminum samples are exposed to air for various periods in order to assess the reaction of PMDI surface and interface between PMDI and aluminum. Figure 10 shows the 106/132 ratios as a function of concentration at different times. When the PMDI concentration decreases, the ratio increases as a result of the dominance of the ion indication of reaction in interface region. As the samples are exposed to atmosphere, the ratio generally increases. For the lower PMDI-concentration samples, however, the 106/132 ratio does not change significantly compared with the higher PMDI-concentration samples. The PMDI reacts with atmospheric moisture on the surface of PMDI layer and the water supply is unlimited, therefore, the PMDI still proceeds to react with water by exposing the samples to air. By contrast, at the interface region, there is a finite amount of hydroxide groups on the aluminum surface so that the water reaction stops after the PMDI has depleted the available hydroxyl groups, and the water reaction at the interface is completed in a short period of time, at least within a few hours.

Specific interaction between MDI and aluminum

Figure 11 shows the high-resolution spectra at mass 102 u for degreased aluminum treated with PMDI at different concentrations, and Table 11 presents the fragments obtained at nominal mass 102 u and their respective assignments. Peak-fitting helps identify a weak peak and/or two peaks close to each other. In this case, peak signals of Al_2O_3^- and AlCHNO_3^- for high concentration PMDI-treated samples (more than 0.25 vol.%) are small and, hence, the presence of the peaks and the peak positions become clear by peak fitting. Additionally, fragments of $\text{C}_2\text{O}_2\text{Na}_2^-$ on degreased aluminum can be identified by knowing the peak position.

The XPS data indicates a 4.1 nm carbonaceous layer on the 0.05 vol.% PMDI-coated aluminum sample. This PMDI layer is thin enough to observe the interface. ToF-SIMS analysis of this interface reveals a mass of 102, which is composed of three components. The lowest mass fragment can be assigned to Al_2O_3^- which originates from the aluminum substrate.^[31] The highest mass fragment can be assigned to $\text{C}_7\text{H}_4\text{N}^-$ which originates from the PMDI adhesive. The intermediate mass fragment is assigned to AlCHNO_3^- which indicates a covalent bond formation between aluminum and PMDI, and the proposed structure of the AlCHNO_3^- fragment is shown in Fig. 12. When the thickness of the PMDI layer increases, the intensities of the AlCHNO_3^- and Al_2O_3^- fragments decrease while the intensity of the $\text{C}_7\text{H}_4\text{N}^-$ fragment increases. On the degreased aluminum sample, the Al_2O_3^- fragment is observed. A second

**Figure 12.** Proposed structure of AlCHNO_3^- fragment.

higher mass fragment is also observed on the neat substrate surface which can be assigned to $\text{C}_2\text{O}_2\text{Na}_2^-$. This is a result of the presence of Na_2O^- , Na_2O_2^- , Na_2^+ and Na_2OH^+ . The distance between AlCHNO_3^- fragment of MDI treated samples and $\text{C}_2\text{O}_2\text{Na}_2^-$ fragment of degreased aluminum is between 7.5 and 11.0 mu, and this is enough to distinguish each fragment. Besides, MDI-treated samples exhibit much low intensities of Na_2O^- , Na_2O_2^- , Na_2^+ and Na_2OH^+ compared with degreased aluminum samples, therefore, $\text{C}_2\text{O}_2\text{Na}_2^-$ fragment can be negligible for MDI-treated samples. Thus, it can be concluded that a fragment assignable to AlCHNO_3^- is present at the interface between PMDI and aluminum, and is characteristic of a specific reaction between the isocyanate and the aluminum substrate.

Conclusion

A study of interface interaction of PMDI and aluminum has been carried out using XPS and ToF-SIMS. The following conclusions can be drawn from the work described in this paper: (i) Water reaction occurs both at the surface of PMDI and at the interface between PMDI and aluminum; (ii) At the interface, there is a limit on the yield of reaction with water because of the finite amount of hydroxyl groups and adsorbed water on the metal surface, and the water reaction is completed within a short period of time. By contrast, the PMDI surface continues to react with water from atmospheric moisture; and (iii) A fragment, indicative of covalent bond formation between PMDI and aluminum (AlCHNO_3^-), was observed at the interface between PMDI adhesive and aluminium substrate.

References

- [1] D. Randall, S. Lee, *The Polyurethanes Book*, John Wiley & Sons Ltd, Chichester, **2002**, pp. 27, 84–86.
- [2] R. G. Dillingham, C. Moriarty, *J. Adhes.* **2003**, 79, 269.
- [3] M. M. Chehimi, J. F. Watts, *J. Adhesion Sci. Technol.* **1992**, 6, 377.
- [4] J. Kim, J. Cho, Y.-S. Lim, *J. Mater. Sci.* **2005**, 40, 2789.
- [5] R. A. De Souza, J. Zehnpfenning, M. Martin, J. Maier, *Solid State Ionics* **2005**, 176, 1465.
- [6] J. F. Watts, A. Rattana, M.-L. Abel, *Surf. Interface Anal.* **2004**, 36, 1449.
- [7] M.-L. Abel, K. Shimizu, M. Holliman, J. F. Watts, *Surf. Interface Anal.* **2009**, 41, 265.
- [8] K. Shimizu, M.-L. Abel, J. F. Watts, *J. Adhes.* **2008**, 84, 725.
- [9] S. Reichlmaier, J. S. Hammond, M. J. Hearn, D. Briggs, *Surf. Interface Anal.* **1994**, 21, 739.
- [10] M.-L. Abel, R. P. Digby, I. W. Fletcher, J. F. Watts, *Surf. Interface Anal.* **2000**, 29, 115.
- [11] G. Beamson, D. Briggs, *High Resolution XPS of Organic Polymers – The Scienta ESCA300 Database*, John Wiley and Sons, Chichester, **1992**, pp. 210–213, 277.
- [12] J. C. Vickerman, *Surface Analysis-The principal Techniques*, John Wiley and Sons, New York, **1998**, pp. 50–52.
- [13] D. Briggs, M. P. Seah, *Practical Surface Analysis by Auger and X-ray Photoelectron Spectroscopy*, John Wiley and Sons, Chichester, **1996**, p. 444.
- [14] C. A. Melendres, S. Van Gils, H. Terry, *Electrochem. Commun.* **2001**, 3, 737.
- [15] S. Van Gils, C. A. Melendres, H. Terry, *Surf. Interface Anal.* **2003**, 35, 387.

- [16] M. R. Alexander, G. E. Thompson, G. Beamson, *Surf. Interface Anal.* **2000**, 29, 468.
- [17] M. R. Alexander, G. Beamson, C. J. Blomfield, G. Leggett, T. M. Duc, *J. Electron. Spectrosc. Relat. Phenom.* **2001**, 131, 19.
- [18] F. Cordier, E. Ollivier, *Surf. Interface Anal.* **1995**, 23, 601.
- [19] Y. Deslandes, G. Pleizier, D. Alexander, P. Santerre, *Polym.* **1998**, 39, 2361.
- [20] J. F. Watts, J. Wolstenholme, *An Introduction to Surface Analysis by XPS and AES*, John Wiley and Sons, Chichester, **2003**, pp. 71, 82–86.
- [21] I. Olefjord, H. J. Mathieu, P. Marcus, *Surf. Interface Anal.* **1990**, 15, 681.
- [22] Safety Data Sheet -SUPRASEC® 5025-, Huntsman PU, Everberg, **2008**, p. 4.
- [23] D. R. Lide, *CRC Handbook of Chemistry and Physics ed. 81st*, CRC Press, Cleveland, **2000**, p. 12, 197.
- [24] P. J. Cumpson, M. P. Seah, *Surf. Interface Anal.* **1997**, 25, 430.
- [25] T. Gruke, *New Advanced in Polymeric MDI Variants EUROCOAT 2002*, Barcelona, Spain, **2002**, p. 3.
- [26] F. W. McLafferty, F. Tureček, *Interpretation of Mass Spectra*, University Science Book, California **1993**, pp. 51–83, 135–282, 293–319.
- [27] M. J. Hearn, D. Briggs, S. C. Yoon, B. D. Ratner, *Surf. Interface Anal.* **1987**, 10, 384.
- [28] N. Nurdin, E. Weilandt, M. Textor, M. Taborelli, N. D. Spencer, P. Descouts, *J. Appl. Polym. Sci.* **1996**, 61, 1939.
- [29] L. A. Pokrajac, M.Sc. Thesis, Fundamental Studies of Polyurethane – Aluminium Adhesion: Phenyl Isocyanate Interaction with Prepared Aluminium Oxide Surfaces, University of Toronto **1998**.
- [30] H. Li, Y. Yan, B. Liu, W. Chen, S. Chen, *Powder Technol.* **2009**, 25, 2875.
- [31] Z. Li, K. Hirokawa, *Appl. Surf. Sci.* **2003**, 220, 136.